Journal of Crystal Growth 310 (2008) 3630–3637

Contents lists available at ScienceDirect

Journal of Crystal Growth

journal homepage: www.elsevier.com/locate/jcrysgro

Structural characterization of single crystals of sodium titanate nanowires prepared by hydrothermal process

R.A. Zárate [a,*], S. Fuentes [a], A.L. Cabrera [b], V.M. Fuenzalida [c]

[a] Departamento de Física, Facultad de Ciencias, Universidad Católica del Norte Casilla 1280, Avenida Angamos 0610, Casilla, Antofagasta, Chile
[b] Facultad de Física, Pontificia Universidad Católica de Chile, Casilla 306, Santiago 22, Chile
[c] Departamento de Física, Facultad de Ciencias Físicas y Matemáticas, Universidad de Chile, Casilla 487-3, Santiago, Chile

ARTICLE INFO

Article history:
Received 3 January 2008
Received in revised form
29 April 2008
Accepted 2 May 2008
Communicated by J.M. Redwing
Available online 18 May 2008

Keywords:
A1. Hydrothermal crystal growth
A1. Nanostructures
A1. X-ray diffraction
A2. Single crystal growth
A2. Titanium compounds

ABSTRACT

$Na_2Ti_6O_{13}$ nanowires have been synthesized using a simple hydrothermal reaction at 130 °C between TiO_2 particles and NaOH aqueous solution. Subsequently the samples were annealed at 500 °C in air for 24 h. Field emission scanning electron microscope(FEG-SEM) and low-magnification transmission electron microscope(TEM) inspection showed wire-like structures with uniform diameters and high contrast, indicating the formation of single crystals. High-resolution transmission electron microscope(HRTEM) and 2-D fast Fourier transform confirmed that the annealed structures correspond to hexatitanate single crystals with diameters between 20 and 120 nm and lengths ranging from 500 nm to 1 μm. Structural characterization was performed by X-ray diffraction(XRD) and Raman spectroscopy. Annealed samples presented diffraction patterns and Raman vibrational spectra corresponding to the sodium hexatitanate indexed as $Na_2Ti_6O_{13}$. FEG-SEM and TEM inspection of the synthesized samples without annealing showed belt- and tube-like structures with diameters between 10 and 60 nm and several micrometers in length. However, their crystalline structure could not be determined using the same techniques applied to the annealed samples.

1. Introduction

Titanates are being extensively studied due to their potential technological applications, such as photocatalysts, fuel cell electrolytes and cation exchangers for the treatment of radioactive liquid waste [1–4], ceramic capacitors, as reinforcing agents of plastic, and as oxygen electrodes for potentiometric gas sensors [5–7]. The physical and chemical properties of titanates depend on synthesis conditions and the preparation method. The standard method used for the synthesis of sodium titanates is solid-state reaction from stoichiometric amounts of Na_2CO_3 and TiO_2, followed by oxidation at temperatures around 1000 °C. This method produces particles around 10 μm in size [8]. The sol–gel method has been used successfully for synthesizing titanates, producing materials with an average size of around 10 μm [5–7]. Solid-state reaction at high temperature has also been used for the synthesis of titanate structures with nanometric dimensions. Xu et al. [9] synthesized sodium hexatitanate nanowires from a mixture of BaC_2O_4, TiO_2 (anatase) and NaCl with a molar ratio of 1:1:20. The mixture was ground with 5 mL of polyglycol ether and was annealed in a furnace at 850 °C for 3 h. Stengl et al. [10] synthesized sodium titanate nanorods through the reaction of commercial nanostructured sodium titanate with ethylene glycol and subsequent heating at 500 and 900 °C. Although is not a titanate, it is worth mentioning that Du et al. [11] synthesized helical potassium hexaniobate nanotubes using a stoichiometric mixture of Nb_2O_5 and K_2CO_3 in an alumina crucible with subsequent heating at 1050 °C.

The hydrothermal process is a powerful method for obtaining titania-based nanotubes or nanowires. This method has the advantage of producing large amounts of material in a single step. It has been used for the synthesis of titanates and niobates. There are reports of the synthesis of potassium titanate nanowires with rectangular cross-section [12] and with good Li-intercalation performance [13]. Sun et al. [1] used the hydrothermal method for large-scale synthesis of sodium and potassium titanate nanobelts. Meng et al. [4] treated hydrothermally pure TiO_2 in the brookite phase with NaOH, leading to sodium hexatitanate nanowires. Yoshida et al. [14] studied the effects of the synthesis conditions and heat treatment on the structure of the ion-exchanged titanate nanotubes, which allowed the crystallization of sodium hexatitanate nanowires and particles with anatase phase. Seo et al. [15] used a single step to synthesize sodium hexatitanate, using a NaOH concentration of 10 M at temperatures between 200 and 250 °C. In this paper, we report on the synthesis of sodium hexatitanate nanowires using a hydrothermal process with pure TiO_2 and NaOH and subsequent annealing at 500 °C.

* Corresponding author. Tel.: +56 55 355517; fax: +56 55 355521.
E-mail address: rzarate@ucn.cl (R.A. Zárate).

0022-0248/$ - see front matter © 2008 Elsevier B.V. All rights reserved.
doi:10.1016/j.jcrysgro.2008.05.020

2. Experimental procedure

The synthesis of sodium titanate was performed hydrothermally in a Teflon beaker containing 25 ml NaOH (Aldrich, 99.99%) at a concentration of 10 M, and placed in a sealed reactor together with 0.21 g of TiO_2 (Aldrich, 99.8%) 50–300 nm in diameter. The resulting solution was stirred for 1 h at room temperature. The mixture was then heated at 130 °C and treated for 18 h. The treated powders were washed with 0.1 M HCl aqueous solution and distilled water, and were then separated from the solution by centrifugation. This procedure was repeated until the washing water showed pH < 7. Subsequently, the samples were annealed at 500 °C for 24 h in air.

The samples were analyzed by X-ray photoelectron spectroscopy (XPS, Physical Electronics model 1257 system) using either the Al anode with energy of 1486.6 eV, or the Mg anode with energy of 1253.6 eV. The XPS peaks were referred to the position of the C1s peak at 284.5 eV. In all XPS measurements the photoelectrons were collected perpendicularly to the surface sample.

The crystallographic structure was characterized by X-ray diffraction. The θ-2θ scans were performed with a Siemens D5000 powder diffractometer with CuKα radiation (40 kV, 30 mA) nonmonochromatized, and by Raman Spectroscopy with a LabRam 010 instrument from ISA using a 633 nm He–Ne laser and no filter at 5.5 mW. Vibrational modes were confirmed by a Confocal Raman Microscope, model CRC200, using 514.5 nm argon laser, from Witec, Ulm, Germany.

The morphology of the samples was examined with a field emission scanning electron microscope (FEG-SEM JSM-6330F) and low vacuum scanning electron microscope (LV-SEM JSM-5900LV), equipped with an energy dispersive X-ray spectroscope (EDX). High resolution images were obtained using a JEOL TEM 3010 operating at 300 kV with a point resolution of 0.17 nm. It is equipped with EDX and selected area electron diffraction (SAED). The samples were ultrasonically dispersed in isopropanol.

3. Results

3.1. Morphology and compositional analysis

Fig. 1a is a FEG-SEM image of the starting anatase material, showing that it consists of spherical particles with dimensions between 50 and 300 nm. After the hydrothermal treatment, the morphology changed completely to wire-like structures, as shown in Fig. 1b. The features of these structures ranged from 10 to 30 nm in diameter and from 500 nm up to several μm in length. As shown in Fig. 1c, the morphology of the samples did not change after annealing in air at 400 °C for 24 h. However, annealing in air

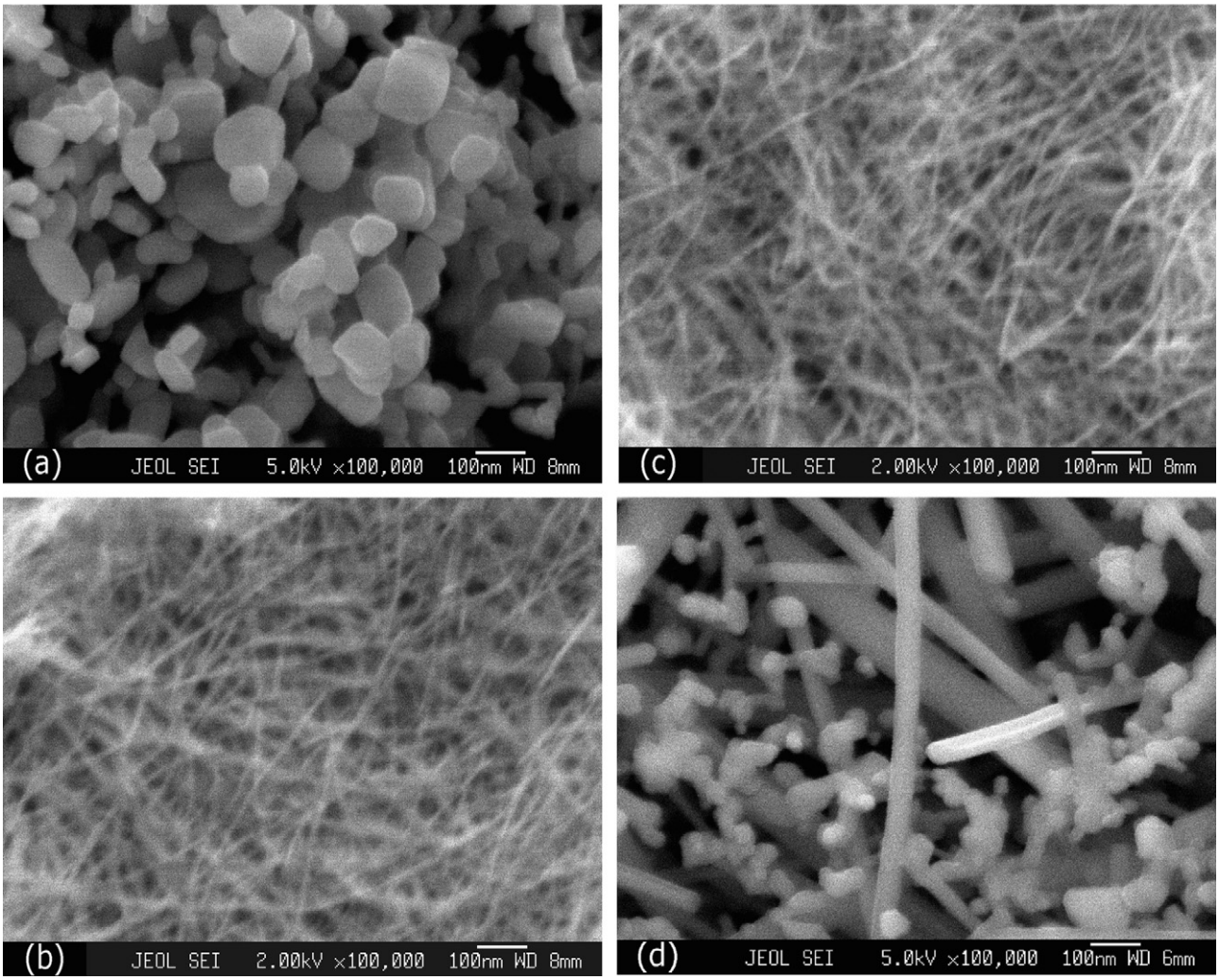

Fig. 1. (a) FEG-SEM image of the starting material, (b) FEG-SEM image of a hydrothermal sample treated at 10 M by 18 h showing wire-like structures, (c) FEG-SEM image of a sample annealed in air at 400 °C and (d) FEG-SEM image of the sample treated at 500 °C for 24 h.

at 500 °C produced a significant change in morphology, as shown in Fig. 1d. These samples were formed by straight wires with attached spherical fine particles. The wires presented a loss of aspect ratio with diameters between 20 and 120 nm and lengths in the range of 1–2 μm, whereas the particle diameter ranged from 20 to about 100 nm.

XPS results are summarized in Table 1, which displays atomic percentages and binding energies from high-resolution XPS spectra. Typical XPS survey is shown in Fig. 2a. The binding energies were obtained after curve fitting with standard procedures. The atomic percentages were obtained from the area under the fitted curve and atomic sensibility factors, with rather large uncertainties in the composition. Within error, the atomic percentages were similar in samples with or without annealing, although both samples are structurally different (see next section). We concluded that the samples do not lose significant amounts of oxygen during annealing, although this element can change its position in the matrix. The difference between the two peaks in O1s lines (labelled as ΔO1s in Table 1) for annealed samples is consistent with that reported for titanate metastable phases in elsewhere [30].

Energy dispersive X-ray spectroscopy (EDX) was used to estimate the atomic percentages in the bulk of the samples, see Table 1. The typical EDX spectra are shown in Fig. 2b. The oxygen atomic percentage of the as-prepared and annealed samples was similar and consistent with the XPS measurements. However, the samples systematically exhibited higher oxygen content than the standard titania and titanates compounds included in Table 1. The sodium content of 6–8% given by EDX was significantly lower than the 17–18% of the XPS estimate, suggesting that the surface of the samples is rich in sodium. In contrast, the surface of the samples is poor in titanium.

3.2. Structure

3.2.1. HRTEM

Fig. 3a is a low-magnification TEM image of a typical sample, synthesized by a hydrothermal process at 130 °C for 18 h without annealing. The image shows several nanotubes of sodium titanate with uniform diameters around 10 nm and lengths from 500 nm up to several μm. The origin of the nanotube-like structures has been attributed to the rolling up of the sheet-like structures by surface forces [16–18]. It has been reported that the rolling up is a very fast event [19,20]. Fig. 3b is a HRTEM image of a nanotube around 8 nm in diameter, which presents many structural defects and non-uniform walls. These two features are indicative of low crystallinity, consistent with the XRD measurements. This nanotube presented intershell distances of about 0.20 nm, calculated after averaging measurements from several zones of this HRTEM image; this distance was confirmed in other HRTEM images not shown. This fringe distance does not correspond to the crystalline planes indexed in the XRD analysis. It is plausible that the as-prepared samples are hydrated nanotubes which can lose water in vacuum when they are exposed to the 300 kV electron beam [16,21]. A bidimensional Fourier transform, shown as an inset in Fig. 3b, display 8 spots caused by four different crystalline orientation and two of them are approximately at 90°. Two crystalline planes have fringe distances about 0.20 nm, whereas the other two have distances slightly higher or smaller.

Fig. 3c is a low-magnification TEM image of a typical sample prepared by a hydrothermal process at 130 °C for 18 h, with annealing. There are several wires with diameters ranging from 20 to 120 nm and lengths ranging from 100 nm to 1 μm. They coexist with spherical particles with diameters ranging from 20 to 100 nm. Fig. 3d is a HRTEM image of a wire 58 nm in diameter displaying a layered structure. A magnified image of the layered structure is shown in the top inset of the same figure. This crystalline structure belongs to the family of $M_2Ti_nO_{2n+1}$, with $n = 3$ or 6 and M being K or Na. $Na_2Ti_6O_{13}$ is a base-centered monoclinic structure with parameters $a = 1.51310$ nm, $b = 0.37450$ nm, $c = 0.91590$ nm and $\beta = 99.3°$ and belongs to the spatial group C2/m [22]. The top inset of Fig. 3d was simulated in a commercial program to obtain the atomic structure of $Na_2Ti_6O_{13}$. The output is shown in Fig. 3e, indicating that the wire grew along the (0 1 0) direction of $Na_2Ti_6O_{13}$, with an interplanar spacing of about 0.74 nm, a value consistent with reports found elsewhere [10,13,14,23]. The wire in Fig. 3d exhibited other sets of intershell spaces of 0.36 and 0.29 nm, corresponding to interplanar distances along the [1 1 0] and [3 1 0] directions of $Na_2Ti_6O_{13}$, respectively. The fast Fourier transform from this wire is shown in the bottom inset of Fig. 3d. The spots can be interpreted as caused by three different crystalline orientations. The uniform diameter and contrast of the wires are properties indicative of single crystal structures [24]. Fig. 3f shows a wire with rounded ends, which are thermodynamically more stable than other structures. Du et al. [12] have performed similar studies on $K_2Ti_6O_{13}$, whose

Table 1
Binding energy, kinetic energy of Auger lines, energy split of the O1s line, and nominal surface atomic percentages (%) of the hydrothermally treated samples

XPS results									
Sample	Atomic percentage			Binding energy (eV)			Auger & Kinetic energy (eV)		ΔO1s (eV)
	Ti2p	O1s	Na1s	Ti2p	O1s	Na1s	Ti LMM	Ti (LMM)	Delta
As-prepared	13	69	18	458.1	529.8 532.1	1017.1	839.7	413.8	2.3
Annealed	14	69	17	458.3	529.9 531.8	1017.4	840.1	413.7	1.9
Anatase				458.0	529.5		838.2	415.3	
EDX results									
As-prepared	26	68	6						
Annealed	24	68	8						
Titania and sodium titanates compounds									
$Na_2Ti_6O_{13}$	28	62	10						
$Na_2Ti_3O_7$	25	58	17						
$Na_2Ti_2O_5 \cdot H_2O$	17	50	16						
$Na_2Ti_9O_{19}$	30	63	7						
TiO_2	33	66	0						

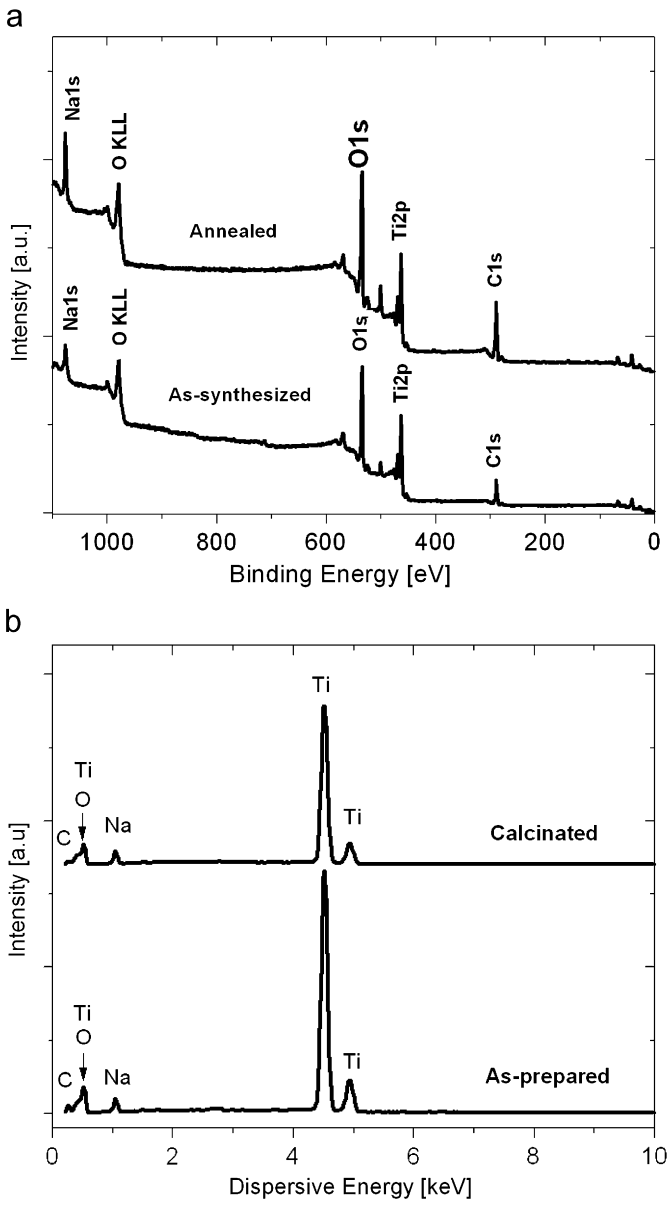

Fig. 2. XPS and EDX spectra of sodium titanate of the as-synthesized and annealed samples: (a) XPS spectrum and (b) EDX spectrum. The samples were prepared in a concentration of 10 M at 130 °C for 18 h of reaction time.

morphology presents rectangular cross-sections. In our case, the wires are perfect cylindrical structures with rounded ends.

Not all $Na_2Ti_6O_{13}$ nanowires grew along their principal directions. As shown in Fig. 4a, some grew along other directions of sodium hexatitanate [23]. In this case the shell distances are around 0.26 nm and correspond to the interplanar distance of the $[\bar{4}\,0\,3]$ planes. The diameter of this wire was estimated at 38 nm from the HRTEM image. Also, one can observe two other sets of crystalline planes with fringe distances of 0.22 and 0.34 nm, which correspond to the distances between $[\bar{5}\,1\,2]$ and $[\bar{1}\,1\,1]$ planes of $Na_2Ti_6O_{13}$, respectively. We performed an exhaustive search and concluded that these distances do not fit any phase of titania [25]. These three sets of planes could correspond to sodium tri- or hexatitanate, but the best fit is with hexatitanate. Using the layered structure of the wire in the top inset of Fig. 4a, we estimated that the angle between the two sets of crystalline planes is around 98.5°. There was a close fit with the angle obtained between $[\bar{4}\,0\,3]$ and $[\bar{1}\,1\,1]$ planes using a commercial computer program, which simulated crystalline structure of the $Na_2Ti_6O_{13}$. On the other hand, no fit was found with the trititanate structure. The bottom inset of Fig. 4a shows the fast Fourier transform of this wire, where the sets of spots again suggest the existence of three sets of crystalline planes.

The HRTEM image of Fig. 4b shows two wires, apparently of different materials. One of them grew along to the $(0\,1\,0)$ direction of $Na_2Ti_6O_{13}$ with shell spaces of about 0.74 nm, while the other is believed to be TiO_2 in the rutile phase. The last nanowire exhibits two sets of fringes separated by about 0.29 and 0.34 nm, corresponding to the distance between $[0\,0\,1]$ and $[1\,1\,0]$ planes of the rutile phase [26]. Fig. 4c shows an anatase single crystal TiO_2 wire with a diameter of about 42 nm. The separation of the fringes in this HRTEM image is 0.35 nm, corresponding to the distance between the $[1\,0\,1]$ planes of the anatase phase. This is consistent with the report by Zhang et al. [27], who also found pure anatase nanowires after similar treatments. Fig. 4d corresponds to an HRTEM image of the spherical particles shown at low magnification in Fig. 3a. This image exhibited a set of shell fringes separated 0.284 nm corresponding to the $[0\,0\,1]$ planes of rutile, and another set of fringes separated an average around 0.70 nm, possibly corresponding to the sodium titanate indexed by $Na_2Ti_9O_{19}$, a phase also reported by Kolenko et al. [28].

3.2.2. XRD

Typical diffractograms of the samples as-prepared, annealed at 400 and 500 °C are shown in Fig. 5. The as-synthesized samples exhibited broad peaks of low intensity, which are difficult to index. However. most likely to index to these samples that they should be metastable compounds (tri and hexatitanates) of the following form of $Na_xH_{2-x}Ti_nO_{2n+1}\cdot mH_2O$ with $0<x<2$ and $n=3$ and 6 [23,29,30,35]. Other researchers have proposed different crystalline phases for the as-synthesized samples, which can be lepidocrocite titanates [16,17] or divalent salt titanate ($Na_2Ti_2O_5\cdot H_2O$) [36,37], etc. However, the crystalline structure of these samples is metastable and contains water and sodium in its matrix, but the exact formulation depends on the synthesis condition and the volume of the sealed or filled factor [38]. In order to synthesize sodium titanate nanowires, the samples should retain the maximum sodium content during the hydrothermal reaction [23,30]. In our case, the samples treated at 10 M and 18 h of reaction have retained the highest quantity of sodium in their matrix. This was proven by the calcination process, which requires temperatures higher than 400 °C to achieve crystallinity. This is indicated by the amorphous character of the sample calcined at 400 °C, as seen in the middle curve in Fig. 5.

The crystallinity of a sample annealed at 500 °C is confirmed by the appearance of many narrow diffraction peaks at the top of Fig. 5. As indicated by the diffraction pattern, this structure is composed mainly of layered sodium titanate indexed as $Na_2Ti_6O_{13}$, mixed with reflections corresponding to anatase and rutile. Yoshida et al. [14] obtained similar results. Their samples were prepared at 120 °C and 10 M for 72 h. In order to decrease the sodium content in their samples, they studied the effects of washing the samples several times with HCl/H_2O and post-heat treatments. They concluded that it was not possible to remove sodium completely. In our work, we found differences between the structural analysis by XRD and HRTEM and the vibrational modes found by Raman spectroscopy. The XRD patterns and HRTEM observation indicated the presence of sodium hexatitanate, anatase and rutile phases, while the analysis by Raman spectroscopy indicated vibrational modes of anatase and sodium hexatitanate.

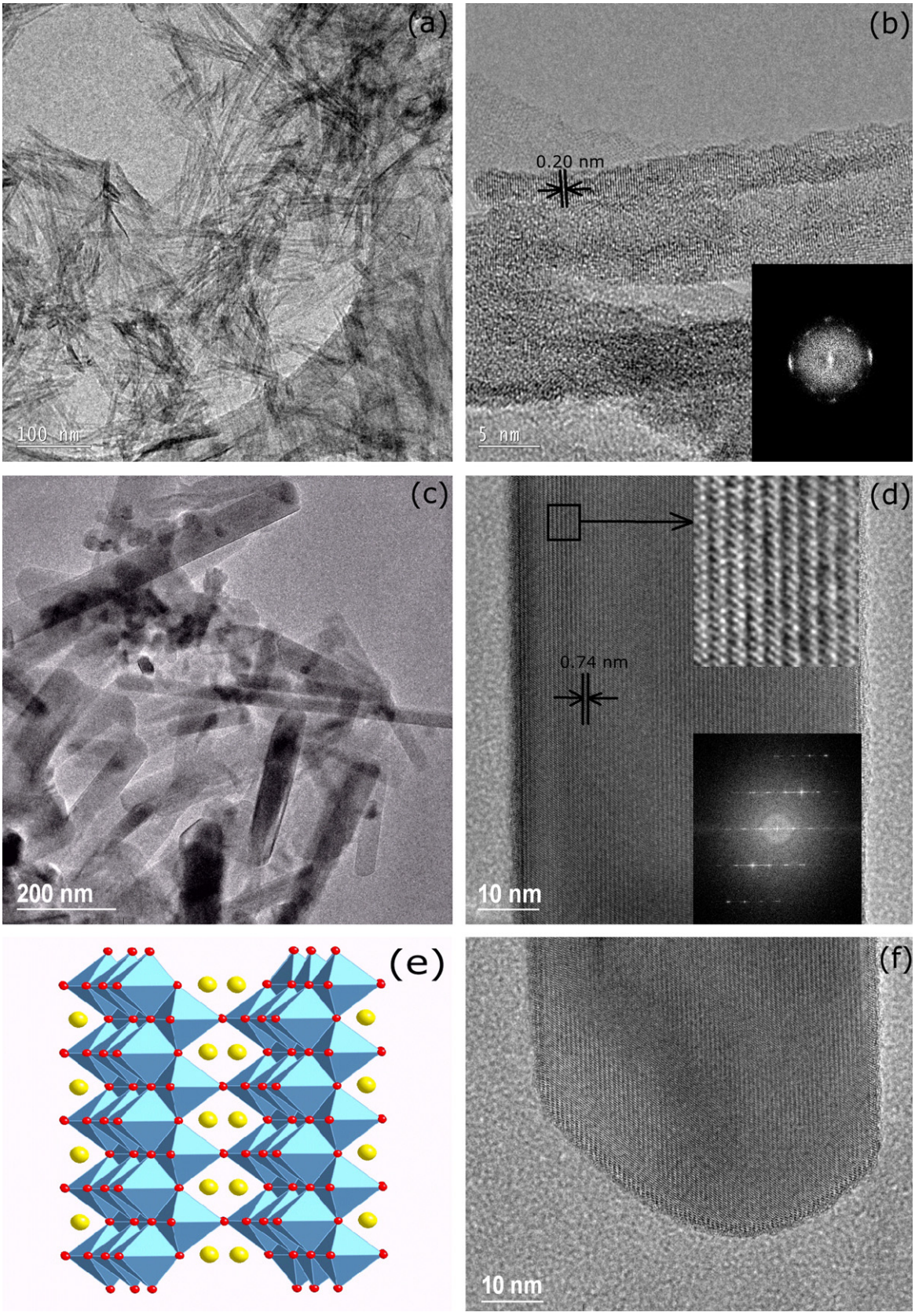

Fig. 3. As-synthesized samples prepared hydrothermally at 10 M for 18 h: (a) Low-magnification TEM image, (b) HRTEM image of the as-prepared samples. Annealed samples at 500 °C for 24 h: (c) Low-magnification TEM image of nanowires, (d) HRTEM image of wire grown along (0 0 1) direction of $Na_2Ti_6O_{13}$, (d) Atomic model of $Na_2Ti_6O_{13}$ along the (0 0 1) direction, and (e) HRTEM image shows the wires have rounded ends. The top inset is an amplification of the image of Fig. 3a and the bottom insets are the bidimensional Fourier transform.

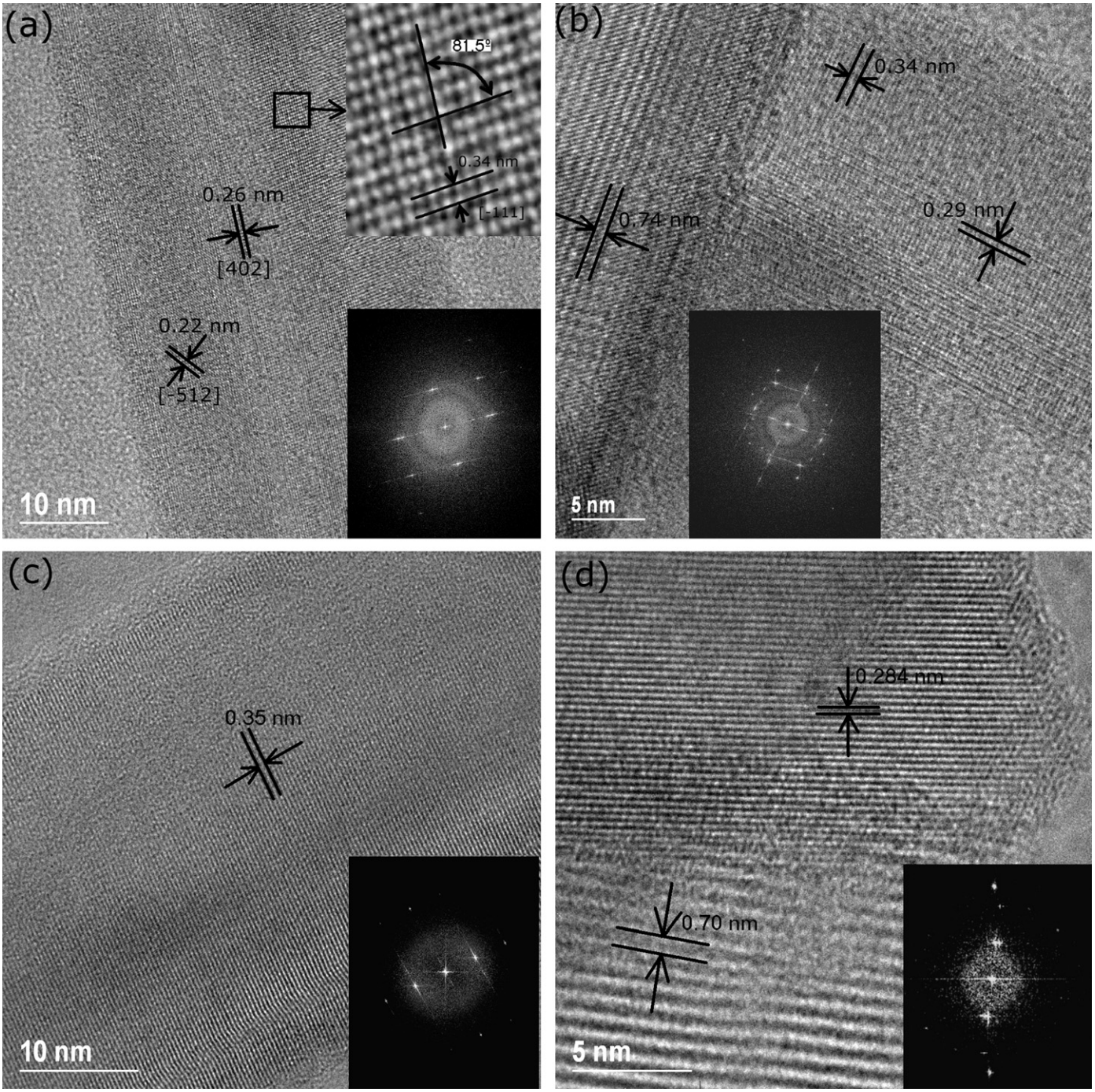

Fig. 4. (a) HRTEM image showing the layered structure of a wire in the $Na_2Ti_6O_{13}$ phase, (b) HRTEM image showing two nanowires with the rutile and sodium hexatitanate phases, (c) HRTEM image showing a single crystal of anatase phase, (d) HRTEM image of spherical particles of rutile and sodium titanate indexed as $Na_2Ti_9O_{19}$ phases. The top inset is an amplification of the image of Fig. 4a and the bottom insets are the bidimensional Fourier Transform.

3.2.3. *Raman spectroscopy*

An independent structural study was performed using Raman spectroscopy. Raman spectra were obtained for the as-prepared and calcined samples and shown in Fig. 6. The as-synthesized samples and those calcined at 400 °C exhibit broad vibration modes not associated with a known structure. Such vibration modes have been observed by several research groups devoted to synthesizing titania-derived nanotubes [10,11,14,30–32,35] and thin films [33,34]. In our work, the as-synthesized samples exhibit better crystallinity than those annealed at 400 °C, which fits with XRD results.

On the other hand, the vibrational modes of the samples annealed at 500 °C are completely different to those bands presented for the as-synthesized samples. Vibrations 165, 193, 222, 247, 274, 329, 363, 408, 455, 477, 608, 677, 741, 869 cm^{-1} correspond to sodium hexatitanate phase, labelled ST, and the other vibrational modes, labelled A, correspond to anatase phase, as shown in the top curves of the Fig. 6. One of the curves at 500 °C shows almost pure vibration modes of ST, whereas the other curve at 500 °C, taken in another region, exhibits mixed bands of ST and anatase. The vibration modes of sodium hexatitanate found in this work are consistent with the research performed by Papp et al.

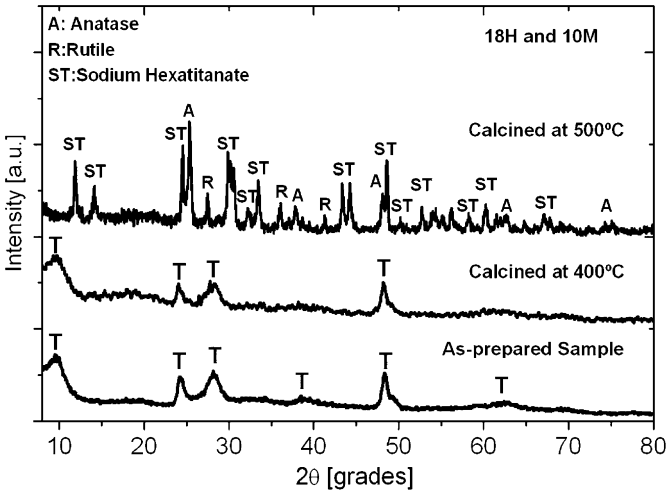

Fig. 5. XRD patterns of samples treated hydrothermally. The bottom curve corresponds to the as-prepared samples; the middle and top to the annealed samples. The samples were prepared at 130 °C in a concentration of 10 M with 18 h of reaction time. A corresponds to the anatase phase, R to the rutile phase, and ST to sodium hexatitanate phases.

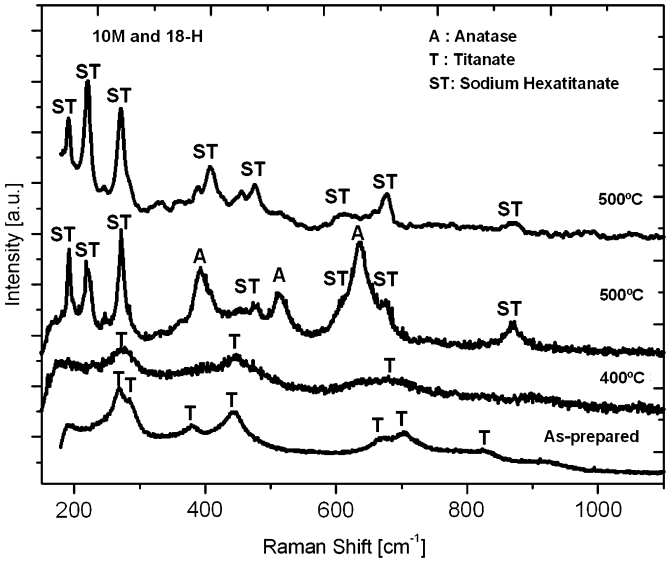

Fig. 6. Loss energy Raman spectra of samples treated hydrothermally. The bottom curve corresponds to the as-prepared samples, and the other curves correspond to samples annealed at different temperatures.

[8], except for the bands. They determined that their bands corresponded to sodium tri and hexatitanate microcrystallites as a function of temperature using Raman spectroscopy and XRD. The bands mentioned by Kolen'ko et al. [28] and Meng et al. [4] at 279 and 309 cm^{-1} did not appear in our work. They argued that those bands corresponded to Na–O–Ti stretching vibrations. The band at 920 cm^{-1} is related to the stretching vibration of short Ti–O bond distorted TiO_6 octahedral involving non-bridging oxygen coordinated with sodium ions [28]. This line found in Refs. [4] and [21], it was not observed in our work nor in Papp's work.

4. Conclusions

In this work we have presented a detailed structural characterization of sodium titanate nanowires grown by a single hydrothermal reaction at 130 °C among particles of pure TiO_2 and NaOH aqueous solution. The characterization of the as-prepared and annealed samples was performed by a battery of analytical techniques: HRTEM, FEG-SEM, XRD, XPS and Raman spectroscopy.

The as-synthesized samples presented tube-like structures and exhibited a hydrated metastable phase, which is very difficult to index. Samples treated at 10 M for 18 h of reaction had the highest sodium content in the matrix, around 6% in atomic percentage, which was very important in the preparation of sodium hexatitanate nanowires after annealing. HRTEM and electron diffraction of the as-synthesized samples presented controversy with XRD, as the electron beam in the TEM technique produced desorption of water in the samples. On the other hand, the uniformity of the nanowires and high contrast observed by FEG-SEM and low-magnification TEM of the annealed samples at 500 °C in air for 24 h is indicative of the formation of single crystals. HRTEM and 2-D fast Fourier transform confirmed that samples were composed of single crystals of sodium hexatitanate nanowires. Structural properties obtained by XRD and Raman spectroscopy also confirmed that the annealed samples corresponded to sodium hexatitanate indexed as $Na_2Ti_6O_{13}$.

Acknowledgments

This work was partially supported by DGIP of the Católica del Norte, grant Minera Escondida 2007 and grant ESO-AUI 2007. We would also like to acknowledge the Laboratorio de Microscopia Electrónica (LME) at Laboratorio Nacional de Luz del Sincrotron (LNLS), in Campinas, Brazil, for providing access to the field emission gun scanning electron microscope and high-resolution transmission electron microscopy. We offer our thanks to Mr. Jaime Llanos, Laboratorio Inorgánica, Departamento de Ciencias Químicas y Farmacéuticas, Facultad de Ciencias, UCN. One of them (A.Z.) acknowledges to Fundación Andes for its support to the Experimental Physics, under the grant No C-13876.

References

[1] X. Sun, X. Chen, Y. Li, Inorg. Chem. 41 (2002) 4996.
[2] A.L. Sauvet, S. Baliteau, C. Lopez, P. Fabry, J. Solid State Chem. 177 (2004) 4508.
[3] C. Zhang, X. Jiang, A. Tian, B. Tian, X. Wang, X. Zhang, Z. Du, Colloids and Sufaces A: Physicochem. Eng. 2004, (in press).
[4] X. Meng, D. Wang, J. Liu, S. Zhang, Mater. Res. Bull. 39 (2004) 2163.
[5] J. Maier, M. Holzinger, W. Sitte, Solid State Ionics 74 (1994) 5–9.
[6] Holzinger J. Maier, W. Sitte, Solid State Ionics 86–88 (1996) 1055.
[7] J. Ramirez-Salgado, P. Fabry, Sensors Actuators B Chem. 82 (2002) 34[9]; J. Ramirez-Salgado, Elisabeth D. Jurado, P. Fabry, J. Eur. Ceram. Soc. 24 (2004) 2477.
[8] S. Papp, L. Korosi, V. Meynen, P. Cool, E. Vansant, I. Dekany, J. Solid State Phys. 178 (2005) 1614.
[9] C.Y. Xu, Q. Zhang, H. Zhang, L. Zhen, J. Tang, L.C. Qin, J. Am. Chem. Soc. 127 (2005) 11584–11585.
[10] V. Stengl, S. Bakardjieva, J. Subrt, E. Vecernokova, L. Szatmary, M. Klementova, V. Balek, Appl. Catal. B: Environ. 63 (2005) 20–30.
[11] G. Du, Q. Chen, R. Che, Z. Yuan, L. Peng, Appl. Phys. Lett. 79 (22) (2001) 3702.
[12] G. Du, Q. Chen, P.D. Han, Y. Yu, L. M Peng, Phys. Rev. 67 (2003) 035323.
[13] B.L. Wang, Q. Chen, J. Hu, H. Li, Y.F. Hu, L. Peng, Chem. Phys. Lett. 406 (14) (2005) 95.
[14] R. Yoshida, Y. Suzuki, S. Yoshikawa, Mater. Chem. Phys. 91 (2005) 409.
[15] D. Seo, H. Kim, J. Lee, J. Crystal Growth 275 (2005) e2371.
[16] R. Ma, Y. Bando, T. Sasaki, J. Phys. Chem. B 108 (2004) 2115.
[17] T. Sasaki, R. Ma, S. Nakano, S. Yamauchi, M. Watanabe, Chem. Mater. 9 (1997) 602.
[18] Y. Mao, M. Kanungo, T. Henraj-Benny, S. Wong, J. Phys. Chem. 110 (2006) 702.
[19] G.B. Saupe, C.C. Waraksa, H. Kim, Y.J. Han, D.M. Kaschak, T.E. Maullouk, Chem. Mater. 12 (2000) 1556.
[20] R.E. Schaak, T.E. Maullouk, Chem. Mater. 12 (2000) 3427.
[21] D.E. Díaz-Droguett, V.M. Fuenzalida, Marcela Díaz-Espinosa, G. Solórzano, J. Mater. Sci. 43 (2008) 541.
[22] JPCDS Data of $Na_2Ti_6O_{13}$ is No. 73-1398.
[23] E. Morgado, M. Abreu, O. Pravia, B. Marinkovic, P. Jardim, F. Rizzo, A. Araujo, Solid State Sci. 8 (2006) 888.

[24] Y. Wu, J. Xiang, C. Yang, W. Lu, C.M. Lieber, Nature 430 (2004) 61.
[25] R. Lee Penn, J. Banfield, Am. Mineral. 83 (1998) 1077;
R. Lee Penn, J. Banfield, Am. Mineral. 84 (1999) 871.
[26] C. Ribeiro, C. Vila, D. Stroppa, V.R. Mastelaro, J. Bettini, E. Longo, E.R. Leite, J. Phys. Chem. C 111 (2007) 5871.
[27] Y.X. Zhang, G.H. Li, Y.X. Jin, Y. Zhang, J. Zhang, L.D. Zhang, Chem. Phys. Lett. 365 (2002) 300.
[28] Y. Kolen'ko, K. Kovnir, A. Gavrilov, A. Garshev, J. Frantti, O. Lebedev, B. Churagulov, G. Tendeloo, M. Yoshimura, J. Phys. Chem. B 110 (2006) 4030.
[29] A. Armstrong, G. Armstrong, J. Canales, R. García, P. Bruce, Adv. Mater. 17 (7) (2005).
[30] R. A. Zárate, S. Fuentes, J.P. Wiff, V.M. Fuenzalida, A. L. Cabrera. Phys. Chem. Solids 68.
[31] X. Gao H. Zhu, G. Pan, S. Ye, Y. Lan. F. Wu, D. Song, J. Phys. Chem. B. 108 (9) (2004) 2868.
[32] A. Kukovecz, M. Hodos, E. Horvath, G. Radnoczi, Z. Konya, I. Kiricsi, J. Phys. Chem. B Lett. 109 (2005) 17781.
[33] J. Muyco, J. Gray, T. Ratto, C. Orne, J. McKitrick, J. Frangos, Mater. Res. Symp. Proc. 873E (2005) K11.5.1.
[34] Z. Tian, J. Voigt, J. Liu, B. Mchenzie, H. Xu, J. Am. Chem. Soc. (JACS) 125 (2003).
[35] O.P. Ferreira, Filho Antônio Souza G., Filho Josué Mendes, O.L. Alves, J. Braz. Chem. Soc. 17 (2) (2006) 393.
[36] C. Tsai, H. Teng, Chem. Mater. 18 (2006) 367.
[37] J. Yang, Z. Jin, X. Wang, W. Li, J. Zhang, S. Zhang, Dalton Trans. (2003) 3898.
[38] B. Poudel, W. Wang, C. Dames, J. Huang, S. Kunwar, D. Wang, D. Barnerjee, G. Chen, Z. Ren, Nanotechnology 16 (2005) 1935.